First principles study of adsorbed Cu_n (n=1-4) microclusters on MgO(100): structural and electronic properties.

V. Musolino[1,2], A. Selloni[3,4], R. Car[1,2]
[1] *Institut Romand de Recherche Numérique en Physique des Matériaux (IRRMA), PPH-Ecublens, CH-1015 Lausanne, Switzerland*
[2] *Département de Physique de la Matière Condensée, Université de Genève, 24 quai Ernest-Ansermet, CH-1211 Genève 4, Switzerland*
[3] *Département de Chimie Physique, Université de Genève, 30 quai Ernest-Ansermet, CH-1211 Genève 4, Switzerland*
[4] *II Facolt di Scienze Matematiche Fisiche e Naturali, Universit di Milano, Sede di Como, I-22100 Como, Italy*

(February 1, 2008)

Abstract

We present a density functional study of the structural and electronic properties of small Cu_n ($n = 1, 4$) aggregates on defect-free MgO(100). The calculations employ a slab geometry with periodic boundary conditions, supercells with up to 76 atoms, and include full relaxation of the surface layer and of all adsorbed atoms. The preferred adsorption site for a single Cu adatom is on top of an oxygen atom. The adsorption energy and Cu-O distance are $E_{S-A} = 0.99$ eV and $d_{S-A} = 2.04$ Å using the Perdew-Wang gradient corrected exchange correlation functional. The saddle point for surface diffusion is at the "hollow" site, with a diffusion barrier of around 0.45 eV. For the adsorbed copper dimer, two geometries, one parallel and one perpendicular to the surface, are very close in energy. For the adsorbed Cu_3 , a linear configuration is preferred to the triangular geometry. As for the tetramer, the most stable adsorbed geometry for Cu_4 is a rhombus. The adsorption energy per Cu atom decreases with increasing the size of the cluster, while the Cu-Cu cohesive energy increases, rapidly becoming more important than the adsorption energy.

I. INTRODUCTION

The interaction of metallic clusters with supporting metal-oxide surfaces is a subject of great current interest, because of the numerous technological applications of these systems, e.g. in the field of thin film growth and catalysis [1,2]. Important objectives of these studies are to understand how the atomic and electronic structure of both subsystems are modified through their interaction, as well as the properties of the resulting interface.

In this paper we focus on the adsorption of small $Cu_n (n = 1, 2, 3, 4)$ clusters on the non-polar (100) surface of MgO. This surface has been widely investigated both experimentally and theoretically [1]. At present, all studies agree that the atomic structure of the undefected surface is very close to an ideally truncated bulk, even though, from the electronic structure point of view, it is not completely clear whether the reduced coordination at the surface gives rise to a reduced ionicity and band gap with respect to the bulk.

Interest in metal clusters has grown remarkably in the past few years. A major question has been to understand the dependance of atomic and electronic structures on cluster size and their evolution from the small cluster regime to the bulk. In particular, copper clusters have been extensively studied, both experimentally and theoretically. As Cu is characterized by a closed d-shell and a single valence electron, an important issue has been to investigate similarities and/or differences between Cu_n and simple alkali-metal clusters. Theoretical work has been done at different levels [3–7] and the properties of small Cu_n ($n = 1, 5$) clusters are now quite well understood.

Studies of Cu clusters and/or overlayers on MgO(100) are not numerous. While most studies conclude that the preferred Cu binding site is on top of a surface oxygen and that the Cu-surface charge transfer is very small, controversial results have been obtained on the fundamental issue of the Cu-surface bond strength. Experimentally, measurements of the initial sticking probability S_0 by medium energy ion scattering (MEIS) [8] have yielded $S_0 \sim 0.5$ at room temperature, which has been interpreted in terms of weak adsorption of Cu adatoms on the MgO surface. More recently, however, a substantially larger value of S_0, ~ 0.82, has been obtained by thermal desorption(TD) techniques [9]. Theoretically, early Hartree-Fock calculations [10] found that Cu binds strongly at

Mg vacancy sites, while the binding with an undefected surface at the oxygen site is very weak (0.2 eV). By contrast, more recent Local Density Functional (LDF) calculations found a rather strong reactivity of the undefected surface, with an adsorption energy of 1.4 eV for an isolated Cu adatom [11] at the oxygen site. Similar LDF computations for the Cu/MgO(100) interface [12] yielded a work of adhesion of 1.0 eV. However, gradient-corrected density functional cluster calculations [13] found that the binding of a single Cu atom at the oxygen site is about 0.3 eV. It appears that the uncertainty in the value of the adsorption energy is so large that even the character of the Cu-surface bonding is unclear. In fact, while adsorption energies of the order of 1 eV or larger suggest a (weak) covalent bond, a polarization mechanism should be primarily involved in the case of binding energies of the order of 0.2-0.3 eV.

In this paper we address this issue by means of first principles density functional calculations within the framework of the Car-Parrinello approach [14]. Our calculations employ a slab geometry with periodic boundary conditions, and, in order to avoid spurious interactions between periodic images of the adatom(s), large supercells (up to 76 atoms) are considered. Moreover, full relaxation of the surface layer and of the adsorbed atoms is allowed for (without symmetry constraints). Our results show that theoretical predictions of the Cu-MgO binding energy based on density functional calculations are quite sensitive to the choice of the exchange-correlation functional. On the basis of our most reliable calculations, which use a gradient-corrected functional known as the Generalized Gradient Approximation [15], the binding energy for a Cu adatom on top of an oxygen of the undefected surface is close to 1.0 eV. Moreover analysis of the electronic charge distribution confirms the occurrence of a weak covalent bond between the Cu3d/4s states and the O2p orbitals. The barrier for the Cu adatom to jump between neighboring binding sites is ~ 0.45 eV, suggesting a substantial mobility of the adatom at room temperature.

Well defined trends show up in the dependence of energetic, structural and electronic properties on the size of the adsorbed cluster. In particular we find that the adsorption energy per atom decreases with increasing the size of the cluster, while the Cu-Cu cohesive energy increases, and large adsorbed clusters are energetically more stable than smaller ones. Thus Cu_n clusters do not dissociate, but rather tend to maintain their identity when adsorbed on the surface. We also infer that Cu atoms which are deposited on the surface at room (or higher) temperature by thin-film growth techniques will tend to aggregate and readily form larger clusters. Moreover, calculations for Cu_5 and larger adsorbed clusters (to be reported in detail elsewhere [16]) indicate a clear preference for 3D over 2D geometries. In this context, it may be interesting to remark that experiments [17,18] indicate that the growth mechanism for Cu on MgO(100) is Stranski-Krastanov, i.e. three-dimensional islands are present on top of a full monolayer.

The layout of this paper is the following. In section II we give the details of our calculations. In section III, after presenting some convergence tests, we discuss atomic structures and energetics. Section IV deals with electronic properties. Both these sections are divided into three main parts. We first discuss the clean MgO(100) surface (sections III B, and IV A), we then consider the free clusters (sections III C and IV B), and finally we deal with the adsorption of copper clusters on the surface in sections III D and IV C. Both sections III and IV end with comments on observed trends in the structural/energetical (III D 5) and electronic (IV C 3) properties. A brief summary and conclusions are given in section V.

II. COMPUTATIONAL DETAILS

Calculations were carried out within the Car-Parrinello [14] approach using both the Local Density (LDA) [19,20] and the Generalized Gradient (GGA) [15] approximations. For a few calculations, we used also the so-called Becke exchange-only functional [21,22], where gradient corrections are applied only to the exchange. For the LDA exchange-correlation energy, we employed the Perdew-Zunger parametrization [23] of Ceperley and Alder's [24] electron-gas results. For the GGA exchange-correlation energy, we used the functional given in Ref. [15]. Unless mentioned, the GGA was applied perturbatively, i.e. the total energy was calculated with the LDA charge density. This non-self-consistent approach to GGA calculations has been shown to yield energies which are usually in excellent agreement with fully-self-consistent GGA calculations (see, e.g., Ref. [15]).

Valence-core interactions were described via Vanderbilt [25] pseudopotentials for O and Cu and Bachelet-Hamann-Schlüter [26] in the Kleinmann-Bylander [27] form for Mg. Pseudopotential cutoff radii were 1.5 and 2.0 a.u. for O and Cu respectively. For Cu, valence electrons included the 3d and 4s shells. Pseudopotentials were always consistent with the approximation used in the density functional calculations, i.e. GGA pseudopotentials for self-consistent GGA and LDA pseudopotentials otherwise (see e.g. Ref. [28]). The smooth part of the electronic wave-functions was expanded in plane-waves with a cut-off of 16 Ry. Tests using a higher cutoff of 20 Ry were performed (see below). A cutoff of 150 Ry was used for the augmented electron density [19,25]. As the supercells that we used were quite large, the k sampling was restricted to the Γ point.

The simulated systems were enclosed in cubic or orthorhombic cells of sizes ranging from 6 to ~ 20 Å with periodic boundary conditions (PBC). In all our calculations, we first performed an electronic minimization with steepest-descent and/or damped dynamics algorithms to bring the electrons in the ground state corresponding to a given initial atomic configuration. We then relaxed the ions with a coupled electronic and ionic damped dynamics. We used the preconditioning scheme of Tassone *et al.* [29] to increase the simulation timestep. Timesteps were in the $1.0 - 1.4 \cdot 10^{-4}$ ps range with a fictitious electronic mass $\mu = 1000$ a.u..

As a first test of the accuracy of our computational scheme, we calculated the equilibrium distance (d) and the vibrational frequency (ν) of a few molecules relevant to our study, namely Cu_2, CuO, and MgO. The results, summarized in Table I, are in very good agreement with the experiment. We also determined the equilibrium lattice constant a and the bulk modulus B of bulk MgO. For these calculations cubic supercells with 64 atoms were used with only Γ k-sampling. Also in this case, our results for a and B are close to the experimental values (see Table II).

III. STRUCTURE AND ENERGETICS

A. Convergence tests

Surfaces were modelled using a repeated slab geometry with periodic boundary conditions parallel to the surface. A vacuum of thickness d_V is introduced between slabs. d_V should be large enough to avoid spurious interactions between slabs. Each slab is composed of N_L layers, and surface supercells containing $(N_{at}/2)$ magnesium and $(N_{at}/2)$ oxygen atoms per layer are used. In our structural optimizations, the lower surface of the slab was kept fixed in a bulk-terminated configuration, while other layers were fully relaxed.

Tests with different values of d_V, N_L and N_{at} were performed for a few selected properties. In Table III the results of these tests for the surface energy E_{surf}, the binding energy E_{S-A} of a single adsorbed copper atom at the on-top oxygen site (see Eq. 2), and the diffusion barrier E_{diff} of a single adsorbed copper atom are reported. E_{diff} is defined as the difference between the Cu-surface binding energies at the absolute minimum (on-top of an oxygen surface atom) and at the saddle point (hollow site, see below). E_{surf} is defined as :

$$E_{surf} = \frac{1}{2A_{cell}}[E^{tot}_{slab} - N_L \frac{N_{at}}{2} E_{bulk}] \tag{1}$$

where E^{tot}_{slab} is the total energy of the slab, E_{bulk} is the energy of an Mg-O pair in the bulk, and A_{cell} is the area of the supercell. The factor 2 accounts for the two exposed surfaces. E_{bulk} was obtained from a bulk calculation using a supercell with 64 atoms.

From Table III, we can see that neither E_{surf}, E_{S-A} nor E_{diff} depend significantly on d_V . E_{surf} depends weakly on N_L, whereas it depends strongly on N_{at}, i.e. on the size of the supercell. This is in turn equivalent to a dependence on the k-sampling of the surface Brillouin zone (larger supercells corresponding to improved sampling). The variation of E_{diff} with N_L and N_{at} is very small. The behavior of E_{S-A} is slightly more complicated, but we can see that also this quantity is very stable when large enough supercells are used.

In Table III results of convergence tests with respect to the plane-wave energy cut-off E^w_{cut} are also reported. We note no substantial change bewteen the 16 Ry and the 20 Ry results for E_{diff} and E_{S-A} (in the case $N_{at} = 18$). Thus, we take $E^w_{cut} = 16$ Ry as our standard energy cut-off. On the basis of these tests, we estimate that our calculated energy differences are accurate within 0.1 eV.

B. Clean MgO surface

Before studying copper adsorption on MgO, we start by a characterization of the clean surface. The structure of the fully relaxed surface is very close to the ideal one, as reported in other works [30,31]. We find an inward surface relaxation of 1.2 % of the bulk inter-layer spacing (0.02 Å). This is accompanied by a rumpling of 1.5%, with an outward displacement of the oxygens with respect to the magnesium atoms. Our best estimate for the surface energy is 1.04 J/m^2 within the LDA (see Table III). This value agrees with the results of previous theoretical work [30,32]. The GGA leads to a remarkable decrease of the surface energy, resulting in $E_{surf} = 0.86$ J/m^2. A similar effect of GGA vs LDA has been found in recent work on SnO_2 and TiO_2 surfaces [33].

C. Free Cu_n clusters

Cohesive energies and average distances for free clusters relevant to the present study are reported in Table IV (see also Fig. 1). The calculations were performed placing the clusters in periodically repeated cells of sizes equal to the ones used for the adsorbed systems. The optimized structures of these clusters were obtained starting from the geometries of the adsorbed clusters on the surface. Thus these structures generally correspond to a local minimum in the potential energy surface. The cohesive energy of the free clusters is calculated as:

$$D_0[n] = -E_{Cu_n} + nE_{Cu_1} \ ,$$

where E_{Cu_n} is the total energy of the cluster with n atoms. The energy of the free copper atom, E_{Cu_1}, was determined using the same pseudopotential and plane wave cut-off employed for the cluster. To account for polarization effects due to the unpaired electron in the atomic $4s^1$ state, we used the empirical correction $\Delta E_{LDA-LSD} = -0.18\ eV(n_\uparrow - n_\downarrow)^2$ [34], where $n_\uparrow$ ($n_\downarrow$) is the number of spin up (down) electrons. Our values for D_0 agree very well with those of other theoretical works and experiments (see Table IV). The general trend for D_0 is to increase as n does. Bonding distances are well reproduced. The most stable geometry is the obtuse triangle for $n = 3$ and the rhombus for $n = 4$.

D. Supported clusters

In this section we present our results for the structure and energetics of supported Cu_n clusters of sizes $n = 1, 2, 3$ and 4 . The energetics will be characterized in terms of two quantities:
1. The cluster adsorption energy with respect to the substrate, E_{S-A} :

$$E_{S-A}[n] = -[E^{ads}_{Cu_n} - E_{slab} - E^{free}_{Cu_n}]/n \tag{2}$$

where $E^{ads}_{Cu_n}$ is the total energy of the adsorbate-substrate system, E_{slab} is the energy of the clean surface, and $E^{free}_{Cu_n}$ is the energy of the "free" cluster. As mentioned above, this energy is obtained by optimizing the structure of the cluster starting from the geometry of the adsorbed cluster on the surface.
2. The intra-cluster binding energy E_{A-A} :

$$E_{A-A}[n] = -[E^{ads}_{Cu_n} + (n-1)E_{slab} - n\ E^{ads}_{Cu_1}]/n \tag{3}$$

where $E^{ads}_{Cu_1}$ is the total energy for the surface with one adsorbed adatom.

The structure of the cluster will be characterized in terms of the average adsorbate-substrate distance $\overline{d}_{S-A}$, the average copper-copper distance $\overline{d}_{A-A}$ and the angle α between an adsorbed copper atom, its supporting oxygen atom and the underlying magnesium atom.

All the results for the following sections are summarized in Table V. As the results for a single adsorbed copper atom show that the on-top oxygen site is strongly favored (see below), we choose to adsorb the cluster atoms at oxygen sites.

1. Cu_1

We considered three possible adsorption sites for a single copper atom on MgO(100): on top of the oxygen site, on top of the magnesium site and between two oxygen sites (hollow site, see Fig. 2). The preferred site is on top of the oxygen atom (see Table V). In the LDA we find an adsorption energy of 1.46 eV and an adsorption distance of 1.89 Å . The oxygen atom is attracted towards the Cu adatom and moves up by 0.1 Å with respect to the other oxygen atoms of the topmost layer. The (LDA) interpolated potential energy surface for the Cu adatom is shown in Fig. 3. The on-top-O site is the only minimum, magnesium is a maximum, while the hollow site is a saddle point and thus corresponds to the transition state for diffusion. The diffusion barrier is $E_{diff} = 0.45$ eV. Assuming a simple Arrhenius-like expression for the adatom attempt-to-jump frequency Γ, with a typical prefactor $\Gamma_0 \sim 10$ THz, we can estimate that at room temperature $\Gamma \sim \Gamma_0 \exp(-E_{diff}/kT) \sim 280$ KHz, i.e. a residence time of 3.6×10^{-6} s. This indicates that Cu adatom motion should be readily seen, for instance in Scanning Tunneling Microscopy (STM) experiments. Following Ref. [35], we can approximately define the temperature for which the adatom diffusion becomes active (i.e. adatoms jump at least once per second) as

$$T_d = \frac{E_{diff}}{k_B\ ln(4D_0/a^2)} \ ,$$

where D_0 is the prefactor in the diffusion coefficent and a (~ 3 Å) is the distance between neighboring adsorption sites. When diffusion can be assimilated to a random walk (i.e. for $E_{diff} \gg k_B\, T$), Γ_0 is related to D_0 [36]. With $\Gamma_0 \sim 10$ THz, $D_0 \sim 2.3 \times 10^{-3}$ cm^2/s, and thus $T_d \sim 180$ K (with an error margin of around 20 K, corresponding to an error of one order of magnitude in D_0). This value of T_d has been confirmed to be of the correct order by recent Electron Energy Loss Spectroscopy(EELS) experiments [37].

As the LDA is known to greatly overestimate binding energies, (fully self-consistent) GGA calculations (also including the optimization of the atomic structure) have been carried out. These lead indeed to a reduction of the adsorption energy of about 0.5 eV, so that the resulting value is $E_{S-A} = 0.99$ eV. Within the GGA, also a significant increase of the Cu-O distance with respect to the LDA takes place (from 1.89 to 2.01 Å). Note however that GGA calculations which employ the LDA charge density and geometry yield a value of the binding energy (0.88 eV) which is very close to that given by the full GGA calculations. For consistency with GGA results for larger clusters, the latter (non self-consistent) value is reported in Table V. From this Table we can also remark that the GGA diffusion barrier is 0.45 eV, i.e. almost equal to that found within the LDA.

Our LDA adsorption energy, adsorption distance and migration barrier agree well with previous LDA calculations [11], whereas there are several important discrepancies between our GGA results and the calculations of Pacchioni and Rösch [13], who used cluster models along with the B-LYP [21,38] exchange-correlation functional. At variance with most available (both experimental and theoretical) results, these authors found that the Mg site is slightly more stable than the on-top O site, while the hollow site is only ~ 0.1 eV higher than the O site. For the latter they obtained $E_{S-A} \sim 0.3$ eV and $d_{S-A} = 2.18$ Å , i.e. values which are much smaller and much larger than our calculated adsorption energy and distance respectively.

There are two main factors which may contribute to the large discrepancies between our results and those of Pacchioni and Rösch. One may be related to the convergence properties of their results with respect to cluster size and embedding. The other is the fact that the exchange-correlation functionals used in the two calculations are different.

In an attempt to check the influence of the latter factor, we performed a (fully self-consistent) calculation using the Becke exchange-only functional (again including the optimization of the atomic structure). We stress that this calculation is only meant to test the dependence of E_{S-A} on the type of gradient corrected functional, since it is widely accepted that the Becke-exchange-only functional is generally less accurate than the GGA (although for many molecules it yields dissociation energies which are in quite good agreement with experiment [39]). Using the Becke functional, we find that the Cu-O adsorption distance becomes 2.09 Å (closer to the value of Ref. [13]), while the binding energy is now extremely low, 0.19 eV *without* spin-polarization correction. This surprising result confirms a tendency to underbind of the Becke exchange-only functional (see, e.g., Ref. [40], where this tendency is found for hydrogen-bonded systems). It also shows that Cu/MgO is a rather "difficult" case, with a strong dependence of the adsorption energy on the choice of the gradient-corrected functional. Although no well-defined experimental value of E_{S-A} is available which may clearly identify the most appropriate functional for the Cu/MgO system, it is important to remark that recent EELS measurements [37] suggest a value of the Cu diffusion barrier which is very close to our result of 0.45 eV, whereas a diffusion barrier of only ~ 0.1 eV is inferred from the calculations of Ref. [13].

2. Cu_2

We considered three different starting geometries for a copper dimer on MgO(100): one with the two Cu's on nearest neighbor O atoms at distance of about 3 Å (A, see Fig. 4); the second (B) having the copper atoms on second neighbor oxygens at distance 4.2 Å , and a magnesium atom in between them; the third (S, Fig. 4) with the copper dimer perpendicular to the surface on top of an O atom.

After optimization, the dimer in configuration A is slightly stretched from its free geometry (from 2.18 Å in the free dimer to 2.25 Å) to satisfy bonding with the O atoms. α is 166°. The oxygen atoms which support the adatoms move by 0.05 Å towards them. The Cu-Cu cohesive energive is of order 0.8-0.9 eV (see Table V). In configuration B, the two copper atoms cannot move as close as they would like to optimize their bond, because of the magnesium atom in between them. The Cu-Cu distance is now 2.34 Å , and the Cu-Cu cohesive energy is decreased accordingly. The two supporting oxygen atoms are displaced from their ideal positions towards the Cu's by rather large amounts, ~ 0.14 Å . Finally in configuration S, the copper dimer bond length is almost identical to that of the free molecule, while the Cu-O distance is the same as that for the adsorbed copper adatom. The molecule is slightly tilted in the (110) plane, the O-Cu-Cu angle being 175°.

Within the LDA, the lowest energy structure is A followed by S (for which the total energy is 0.22 eV higher than for A) and B (+0.33 eV w.r.t. A). Rather unexpectedly, S is found to be the most

stable structure within the GGA, even though the difference with A is quite small: 0.15 eV when the GGA is applied non-selfconsistently, and 0.04 eV only when a fully selfconsistent GGA calculation (including structural optimization) is performed. This indicates a very delicate balance between intradimer cohesion (dominant in the S configuration) and dimer-surface binding (dominant for the A structure).

To investigate this issue further, we sampled the total energy surface as a function of the angle (θ) between the dimer and the surface, in a plane perpendicular to the surface and passing through two neighboring oxygen atoms (the (110) plane). We constrained the value of θ and allowed all the other degrees of freedom to relax. The resulting S→A energy barrier, occurring at $\theta \sim 20^{\circ}$, is $\Delta E^{dimer} = 0.13$ eV (see Fig. 5). Frequent flips between the S and A structures can be thus expected at room temperature.

3. Cu_3

The lowest energy structure for the free Cu_3 cluster is an obtuse triangle, corresponding to a Jahn-Teller distortion of the equilateral triangle [4–6]. By contrast, we find that the linear arrangement on nearest neighbor O sites (configuration A, see Fig. 4) is the preferred adsorption geometry of the copper trimer. It is more bound to the surface and tighter (see the value for $\overline{d}_{S-A}$) than the triangular arrangement (configuration B). This is due to the presence of a magnesium atom on one of the edges of the triangle, which prevents the two copper atoms from binding in an optimal way. In the triangular arrangement, all three copper atoms are tilted towards each other: α is 166° for the central atom and 162° for the other two. The oxygen atoms move only slightly out of their equilibrium positions. In configuration A, the copper atoms at the two ends of the line are tilted towards the middle adatom to achieve optimal Cu-Cu distances ($\alpha = 159^{\circ}$). Oxygen atoms which support copper atoms at the end of the line are attracted to them and move up by 0.08 Å while no difference can be seen for the middle atom.

4. Cu_4

To determine the most stable arrangement of adsorbed Cu_4 , two different starting geometries were considered: a linear configuration on nearest neighbour O atoms (A), and a square geometry with the four Cu's on top of nearest neighbor surface O atoms and a Mg atom at the center of the square (B), similar to one considered by Pacchioni and Rösch [13] (see Fig. 4).

We find that upon relaxation the square changes its shape to a rhombus, which, as in the case of the free Cu_4 cluster [3–5], becomes the lowest energy structure for the adsorbed tetramer. However, the adsorbed rhombus is not perfectly planar : the Cu atoms at the end of the short diagonal attract their supporting oxygens by 0.11 Å ($d_{S-A} = 2.11$ Å) with $\alpha = 154^{o}$, while the other two Cu atoms, staying almost on top of their oxygens, lower them with respect to other surface atoms by 0.07 Å ($d_{S-A} = 2.17$ Å) with $\alpha = 175^{o}$ (see Fig. 4). The adsorption energy per atom of this structure is very low (see Table V), and close to that found by Pacchioni and Rösch [13] for Cu_4 in a square geometry.

Upon relaxation, the linear Cu_4 cluster (~ 0.7 eV higher in energy than the rhombus) splits into two dimers of length 2.28 Å , separated by a distance of 3.28 Å (see Fig. 4). However, these dimers are not totally independant, since they show a mirror plane symmetry with respect to the center of the line: $\alpha = 160^{o}$ for the extreme atoms and $\alpha = 174^{o}$ for the inner atoms. The oxygen atoms supporting the extremity of the line move up by 0.06 Å , attracted by the adsorbate atoms, while the other two lower their positions by 0.02 Å .

5. Trends

Competition between adsorption on the surface and cohesion among the atoms in the cluster is an important feature of the Cu/MgO system. In the $n = 2$ case, the dimer (configurations A and B) is stretched from its equilibrium distance in the gas-phase to take into account interaction with the surface. The balance between intra-dimer and surface-dimer bonding is delicate: in fact full GGA calculations yield very close energies for the A and S (standing) geometries. In the $n = 3$ case, the linear structure is preferred to the triangular arrangement, which is more stable in the gas-phase, because it allows a better bonding to the substrate. For $n = 4$, instead, the rhombus, which is by far the most stable stable isomer in the gas-phase, is also preferred for the adsorbed cluster, in spite of its low adsorption energy. In the $n = 4$ linear case, the cluster prefers to split into two separate dimers in order to optimize its structure and its bonding with the supporting oxygens.

In Fig. 6 our results for the surface-adsorbate (E_{S-A}, c) and d)) and adsorbate-adsorbate intra-cluster (E_{A-A}, a) and b)) binding energies are summarized. We can remark that the effect of gradient corrections is more important on E_{S-A} than on E_{A-A}, and the absolute difference between LDA and GGA results for E_{S-A} tends to reduce with n. With increasing n, the adsorption energy per atom E_{S-A} decreases, while E_{A-A} first decreases (from $n = 2$ to $n = 3$) and then increases. Calculations for $n > 4$ clusters [16] confirm the latter trend. This is an indication that, provided deposition on the surface is sufficiently "soft", Cu_n clusters will tend not to wet the surface but to retain their cluster-like character, particularly in the case of large clusters. Our results also show that larger (adsorbed) aggregates are energetically more stable than smaller ones. Thus when Cu atoms are deposited on the surface to grow a film, at high enough temperature formation of large aggregates by coalescence of small diffusing clusters, particularly monomers, could be observed.

Calculations for $n > 4$ [16] also show that 3D geometries are energetically preferred to 2D ones. In particular for $n = 5$ the lowest energy configuration is a square pyramid ($E_{S-A} = 0.43$ eV, $E_{A-A} = 1.08$ eV, within GGA). The total energy of this configuration is found to be 0.95 eV lower than that of the planar trapezoidal geometry.

IV. ELECTRONIC PROPERTIES

A. Clean MgO surface

The (LDA) density of occupied states (DOS) – obtained by artificially broadening the one-electron eigenvalues with gaussians of width 0.15 eV – is displayed in Fig. 8. This shows oxygen $2s$ (region I) and $2p$ bands (regions II and III) separated into smaller bands.

Since only occupied states are included, magnesium states should not be seen if one considers the MgO(100) surface to be completely ionic and hence the magnesium valence states to be empty. Recent calculations [41] have nonetheless shown that some charge stays on the magnesium instead of going to the oxygens. This is also the case in our study when one looks at the projected DOS of Fig. 9.

The overall bandwidth (difference between the top of the O2p and the bottom of the O2s bands) is 17.0 eV, while the width of the O2p band is 4.0 eV. Corresponding experimental values by Rössler *et al.* [42] are 20.0 and 5-6 eV respectively. We also calculated the bandgap between occupied and empty states and found $E_{gap} = 3.0$ eV, against an experimental value of 7.8 eV [43] for the bulk. The surface band gap has been measured and calculated to be of around 4.5 eV [44] and 5.0 eV [45] respectively. The strong underestimate of the gap is a well-known problem of density functional theory.

B. Free Cu_n clusters

In order to help understanding the bonding mechanism between the Cu_n clusters and the MgO(100) surface, in Fig. 7 we show the DOS of the free clusters obtained by optimizing the adsorbed structures. Similar DOS for Cu_n up to $n = 5$ have been discussed previously by Jackson [5]. Our monomer's DOS shows the small separation between the 4s state (at $\sim$ -4.5 eV) and the 3d state (at $\sim$ -5.5 eV). For the dimer, this split-off state on the high energy side of the 3d band is missing. This indicates that the dimer is a closed-shell system [4]. This characteristics holds also for the Cu_3 and Cu_4 *linear* clusters, whereas a split-off state on the high-energy side of the DOS is present for the *triangular* Cu_3 and for the *rhombus*. The character of the high-energy state is mainly s-like, as found by Jackson [5] and Massobrio *et al.* [3]. In analogy with the work of Li *et al.* [11], we shall call the split-off state $4s^*$.

C. Supported clusters on MgO

In this section we try to elucidate the bonding between the Cu_n clusters and the MgO(001) surface. To this end we shall examine the DOS for the adsorbed clusters as well as the charge density (for the case $n = 1$).

1. Cu_1

The upper panel of Fig. 8 shows the (LDA) DOS for a single copper atom at the oxygen and magnesium sites of the MgO(100) surface. A split-off state appears on the top of the bands (region

IV). This state is well inside the bandgap of the clean MgO(100) surface, and causes its reduction from a value of 3.0 eV for the clean surface to 1.5 eV for the on-top O site. In the magnesium site case, the feature corresponding to the 4s* state is smaller. For the O site, prominent states are present in region II. These states are responsible for the Cu-surface bonding as shown by Li *et al.* and below.

In Fig. 9 we present the s, p, d decomposition of the DOS for copper at the stable adsorption on-top O site. This decomposition was performed by projecting the plane wave basis onto spherical waves centered on the Cu, O, and Mg atoms. Inspection of Fig. 9 shows that the split-off state originates as expected from the Cu4s state. Here no contribution from the d states is present. Regions II and III consist mainly O2p states and Cu3d states, the contribution from the Cu4s state being small but not negligible especially near the band edges. Region I contains almost exclusively O2s states. Magnesium states appear in regions II and III, indicating that the ionicity of the surface might not be complete.

To further investigate the character of the bonding, in Fig. 10 we present plots of the (LDA) charge density for the various spectral regions of the DOS. Here, the contours of the integrated charge density are shown in a plane perpendicular to the surface and containing only O atoms. For technical reasons, the part of the wave functions localized at the cores is missing from the plots. In region I, the charge density has the character of s states centered on the oxygens. The charge is distorted towards the overlying copper atom. In region II, it clearly indicates the presence of a bond through overlap between oxygen 2p and copper 3d/4s states. Region III shows little overlap between oxygen and copper orbitals. In region IV the split-off state has anti-bonding character. In agreement with the LDA calculations by Li *et al.* [11], the above analysis of the charge density indicates that the bonding between a copper adatom and MgO(001) is due to a mixing of the Cu 3d/4s states and the oxygen 2p band. The bonding part lies in region II, while the antibonding counterpart is in region IV.

The fact that the states in region II are those mostly responsible for the Cu-surface bonding is further confirmed by Fig. 11 which compares the DOS for the $n = 1$ case calculated using the LDA, the GGA, and the Becke exchange-only functional. There is clearly a relationship between E_{S-A} and the importance of these bonding states. In fact, the LDA which yields the highest adsorption energy also shows the most prominent features in the DOS, while in the "Becke-only" DOS these peaks are missing.

2. Cu_2, Cu_3, Cu_4

The DOS for the adsorbed dimer shows few closely spaced states near the top of the O-2p band (see Fig. 8). Furthermore, for the standing dimer (S) the density of states in region II is very similar to that of a single copper atom at the on-top-O site. This indicates that the intra-molecular bond is very little perturbed in this case. The closed shell nature of the dimer [4] can explain why it prefers to adsorb vertically on the surface (at the GGA level). This can also explain why the adsorption energy drops by ~ 0.4 eV from $n = 1$ to $n = 2$ (see Fig. 6, c) and d)). At variance with the free-cluster case, for $n = 3$ the linear arrangement (configuration A, see Fig. 4) is preferred to the triangular one (configuration B). As mentioned previously, this can be attributed to the fact that for configuration B an Mg atom is present in between a pair of Cu atoms, thus hindering their bonding. From an electronic point of view, the bonding states in region II are much more prominent for the linear case than for the triangular one. We can also remark the presence of two separate 4s* peaks for the linear arrangement. For $n = 4$, the linear tetramer splits into two dimers (configuration A of Fig. 4) and displays a DOS similar in shape to that of the dimer. A similarity with the linear trimer case can be also noted. For the rhombus a well defined band above the top of the O-2p band is present, while the bonding states in region II are less prominent than for the linear arrangement. Indeed the substrate-adsorbate binding energy E_{S-A} for the rhombus is lower than for the linear tetramer (see Table V). Viceversa, E_{A-A} for the rhombus is substantially larger than for the linear case. This is consistent with the fact that for free Cu_4 clusters the rhombus is much more stable than all other isomers [4].

3. Trends

When n increases, the gap between the 4s^* state and the top of the nearest occupied band is progressively filled; the formation of an independant band is clearly shown in Fig. 8. Another interesting feature is the reduction of the DOS feature corresponding to the bonding states in region II. This is a confirmation of the fact that with increasing their size the adsorbed copper clusters reduce their ability to bond to the surface. Intracluster bonding becomes dominant and the copper agregates thus tend to retain their gas-phase structure.

V. CONCLUSION

This paper reports a first principles study of copper microclusters adsorbed on an MgO(100) surface. At variance with previous calculations where cluster models of rather small size were generally used to represent the surface, in our study we use a slab model and periodically repeated supercells of large size (up to 36 atoms per layer). Moreover full relaxation, without symmetry constraints, of all atoms in the cluster and in the surface layer is allowed for.

In agreement with previous studies, our results show that the preferred site of adsorption for a single Cu adatom on defect-free MgO(100) is the oxygen site. The calculated binding energy and distance are found to depend significantly on the type of gradient corrections used. According to our best estimate, obtained using the GGA, the binding energy is of about 1 eV, suggesting a weak covalent bond. This is confirmed by the character of the electronic charge density, which shows the mixing of copper $3d$ and $4s$ states with oxygen $2p$ orbitals. The Cu hopping barrier is ~ 0.45 eV (largely independent of the functional), suggesting that significant adatom diffusion should be seen starting from ~ 180 K.

When increasing the size of the clusters, we find that the intra-cluster binding energy tends to dominate over the adsorption energy, larger (adsorbed) aggregates being energetically more stable than smaller ones. These results suggest that the clusters which are "softly" deposited on the surface at low temperatures will tend to keep their gas-phase structure (see, e.g., Cu_2 and Cu_4) while optimizing their bonding with the substrate. Viceversa, when Cu atoms are deposited on the surface to grow a Cu film on MgO(100), formation of large aggregates by coalescence of small diffusing clusters (particulary monomers) should be observed at high enough temperature. Results for $n > 4$ (to be presented elsewhere) show that bigger copper clusters tend to form three-dimensional structures instead of planar ones.

VI. ACKNOWLEDGEMENTS

We are very grateful to A. Pasquarello for many helpful discussions and assistance with the Car-Parrinello-Vanderbilt LDA/GGA plane waves code. We are also pleased to thank M.-H. Schaffner, F. Patthey, Prof. W. Schneider, and colleagues at IRRMA for useful discussions. The calculations have been performed on NEC SX-3 and SX-4 machines at the CSCS in Manno, Switzerland, and on a CRAY Y-MP computer at the EPFL in Lausanne, Switzerland. One of us (V.M.) acknowledges the Swiss National Science Foundation for support under Grants No. 20-39528.93 and 20-49486.96.

---

1. For a recent review on metal-oxide surfaces, see V.E. Henrich and P.A. Cox, *The surface science of metal oxides*, Cambridge University Press,1994 Cambridge.
2. M.W. Finnis, J. Phys. : Condens. Matter **8** (1996), 5811.
3. C. Massobrio, A. Pasquarello, and R. Car, Chem. Phys. Lett. **238** (1995), 215.
4. P. Calaminici, A.M. Köster, N. Russo, and D.R. Salahub, J. Chem. Phys. **105** (1996), 9546.
5. K.A. Jackson, Phys. Rev. B **47** (1993), 9715.
6. U. Lammers and G. Borstel, Phys. Rev. B **49** (1994), 17360.
7. O.B. Christensen and K.W. Jacobsen, J. Phys. : Condens. Matter **5** (1993), 5591.
8. J.B. Zhou, H.C. Lu, and T. Gustafsson, Surf. Sci. Lett. **293** (1993), L887.
9. M.-C. Wu, W.S. Oh, and D.W. Goodman, Surf. Sci. **330** (1995), 61.
10. N.C. Bacalis and A.B. Kunz, Phys. Rev. B **32** (1985), 4857.
11. Y. Li, D.C. Langreth, and M.R. Pederson, Phys. Rev. B **52** (1995), 6067.
12. R. Benedek, M. Minkoff, and L.H. Yang, Phys. Rev. B **54** (1996), 7697.
13. G. Pacchioni and N. Rösch, J. Chem. Phys. **104** (1996), 7329.
14. R. Car and M. Parrinello, Phys. Rev. Lett. **55** (1985), 2471.
15. The name GGA is generally used to indicate the approximation developed by Perdew and Wang, reported in: Perdew, J.P.; Chevary, J.A.; Vosko, S.H.; Jackson, K.A.; Pederson, M.R.; Singh, D.J.; Fiolhais, C., Phys. Rev. B **46** (1992), 6671.
16. V. Musolino *et al.*, to be published.
17. J.-W. He and P.J. Møller, Surf. Sci. **178** (1986), 934.
18. I. Alstrup and P.J. Møller, Appl. Surf. Sci. **33/34** (1988), 143.
19. K. Laasonen, A. Pasquarello, R. Car, C. Lee, and D. Vanderbilt, Phys. Rev. B **47** (1993), 10142.
20. A. Pasquarello, K. Laasonen, R. Car, C. Lee, and D. Vanderbilt, Phys. Rev. Lett. **69** (1992), 1982.
21. A.D. Becke, Phys. Rev. A **38** (1988), 3098.
22. A.D. Becke, J. Phys. Chem. **96** (1992), 2155.

23. J.P. Perdew and A. Zunger, Phys. Rev. B **23** (1981), 5048.
24. D.M. Ceperley and B.J. Alder, Phys. Rev. Lett. **45** (1980), 566.
25. D. Vanderbilt, Phys. Rev. B **41** (1990), 7892.
26. G.B. Bachelet, D.R. Hamann, and M. Schlüter, Phys. Rev. B **26** (1982), 4199.
27. L. Kleinmann and D.M. Bylander, Phys. Rev. Lett. **48** (1982), 1425.
28. A. Dal Corso, A. Pasquarello, A. Baldereschi, and R. Car, Phys. Rev. B **53** (1996), 1180.
29. F. Tassone, F. Mauri, and R. Car, Phys. Rev. B **50** (1994), 10561.
30. S. Pugh and M.J. Gillan, Surf. Sci. **320** (1994), 331.
31. J.B. Zhou, H.C. Lu, T. Gustafsson, and P. Häberle, Surf. Sci. **302** (1994), 350.
32. M.P. Tosi, Solid State Phys. **16** (1964), 1.
33. J. Goniakowski, J.M. Holender, L.N. Kantorovitch, M.G. Gillan, and J.A. White, Phys. Rev. B **53** (1996), 957.
34. Y.-M. Juan and E. Kaxiras, Phys. Rev. B **48** (1993), 6376.
35. R. Stumpf and M. Scheffler, Phys. Rev. Lett. **72** (1994), 254.
36. G. Boisvert and L. Lewis, Phys. Rev. B **54** (1996), 2880.
37. M.-H Schaffner, F. Patthey, and W.D. Schneider, private communication.
38. C. Lee, W. Yang, and R.G. Parr, Phys. Rev. B **37** (1988), 785.
39. A.D. Becke, J. Phys. Chem. **97** (1992), 9173.
40. M. Sprik, J. Hütter, and M. Parrinello, J. Phys. Chem. **105** (1996), 1142.
41. U. Schönberger and F. Aryasetiawan, Phys. Rev. B **52** (1995), 8788.
42. D.M. Rössler and W.C. Walker, Phys. Rev. **159** (1967), 733.
43. R.C. Whited, C.J. Flaten, and W.C. Walker, Solid State Commun. **13** (1973), 1903.
44. L.H. Tjeng, A.R. Vos, and G.A. Sawatzky, Surf. Sci. **235** (1990), 269.
45. V.-C. Lee and H.-S. Wong, J. Phys. Soc. Jpn. **45** (1978), 895.
46. Radzig and Smirnov, *Reference Data on Atoms, Molecules, and Ions*, Springer Verlag, Berlin, 1985.
47. Huber and Herzberg, *Constants of Diatomic Molecules*, Van Nostrand Reinhold Company, New York, 1979.
48. M. Causà, R. Dovesi, C. Pisani, and C. Roetti, Phys. Rev. B **33** (1986), 1308.
49. E.S. Gaffney and T.J. Ahrens, J. Chem. Phys. **51** (1969), 1088.
50. O.L. Anderson and Jr. P. Andreatch, J. Am. Ceram. Soc. **49** (1966), 404.
51. G. Peckham M.J.L. Sangster and D.H. Saunderson, J. Phys. C **3** (1970), 1026.
52. R.L. Clendenen H.G. Drickhamer, R.W. Lynch and E.A. Perez-Albuerne, Solid State Physics (New York) (F. Seitz and D. Turnbull, eds.), vol. 17, Academic, New York, 1966, p. 13.
53. E.A. Rohlfing and J.J. Valentini, J. Chem. Phys. **84** (1986), 6560.
54. W. Weltner and R.J. Van Zee, Ann. Rev. Phys. Chem. **35** (1984), 291.

TABLE I. Calculated (LDA) bond distances and stretching frequencies of a few selected molecules.

Molecule	d [Å]		ν [eV]	
	LDA	Exp. [46,47]	LDA	Exp. [46,47]
Cu_2	2.18	2.22	0.034	0.033
CuO	1.69	1.72	0.087	0.079
MgO	1.77	1.75	0.103	0.097

TABLE II. Calculated structural parameters for bulk MgO. a is the lattice constant, B is the bulk modulus, V_0 and B' are parameters from the Murnhagen equation of state.

			a [Å]	B [Mbar]	V_0 [Å^3]	B'
This work	(LDA)	Murnhagen fit	4.25	1.63	68.74	3.70
	(LDA)	Polynomial fit	4.25	1.57	68.63	-
Theory	(Hartree-Fock)	Ref. [48]	4.20	1.86	66.18	3.53
Exp.	-	Ref. [49–52]	4.21	1.55-1.62	66.60	-

TABLE III. Convergence tests for the surface energy (E_{surf}), the Cu-surface binding energy (E_{S-A}) and the Cu diffusion barrier (E_{diff}). Calculations are within the LDA. N_L is the number of layers, N_{at} is the number of atoms per layer, d_v is the width of the vacuum. E^w_{cut} is the energy cut-off for the smooth part of the wave-functions.

N_L	N_{at}	E^w_{cut} [Ry]	d_v [Å]	E_{surf} [J/m^2]	E_{S-A} [eV]	E_{diff} [eV]
2	8	16	7.4	1.59	1.71	-
3	8	16	7.8	1.60	1.29	0.53
3	8	16	19.8	1.77	1.25	0.51
3	8	20	13.8	-	1.50	0.53
2	18	16	12.8	1.19	1.46	0.45
2	18	20	12.8	-	1.50	-
3	18	16	10.7	1.19	1.48	-
2	36	16	12.8	1.04	-	-

TABLE IV. Cohesive energy per atom (D_0/n) and average Cu-Cu distance for the free clusters shown in Fig. 1. The values for the cohesive energy have been obtained within the GGA(LDA). Spin-polarization effects are included in the works of Jackson and Calaminici *et al.*, but not in that of Lammers *et al.*.

n	Geometry	Ref.	D_0/n [eV]	$\overline{d}$ [Å]
2	Line	This work	1.13 (1.33)	2.18
2	Line	Jackson [5]	1.08 (1.36)	2.18
2	Line	Calaminici *et al.* [4]	1.13 (1.30)	2.20
2	Line	Exp [47,53]	1.04	2.22
3	Obtuse triangle (C_{2v})	This work	1.13 (1.43)	2.31
3	Obtuse triangle (C_{2v})	Jackson [5]	1.16 (1.52)	2.27
3	Obtuse triangle (C_{2v})	Calaminici *et al.* [4]	1.12 (1.34)	2.34
3	Obtuse triangle (C_{2v})	Exp. [54]	1.02	-
3	Line	This work	1.10 (1.36)	2.23
3	Line	Lammers *et al.* [6]	0.57	-
3	Line	Calaminici *et al.* [4]	1.18 (1.48)	2.27
4	Rhombus (D_{2h})	This work	1.53 (1.89)	2.32
4	Rhombus (D_{2h})	Jackson [5]	1.52 (1.95)	2.30
4	Rhombus (D_{2h})	Lammers *et al.* [6]	1.04	-
4	Rhombus (D_{2h})	Calaminici *et al.* [4]	1.59 (1.90)	2.36
4	Line	This work	1.48 (1.74)	2.24

TABLE V. Calculated energies (in eV) and structures (distances in Å) for adsorbed copper clusters shown in Fig. 4. All GGA results in this Table are from non-selfconsistent calculations which employ the LDA charge density and geometry.

		LDA		GGA		LDA	LDA
n	Geometry	E_{S-A}	E_{A-A}	E_{S-A}	E_{A-A}	$\overline{d}_{S-A}$	$\overline{d}_{A-A}$
1	On top of O	1.46	-	0.88	-	1.89	-
1	On top of Mg	0.45	-	0.18	-	2.51	-
1	Hollow	1.01	-	0.43	-	2.07	-
2	O-Cu-Cu-O (A)	1.07	0.93	0.58	0.83	1.99	2.25
2	O-Cu-Mg-Cu-O (B)	0.90	0.77	0.47	0.72	2.11	2.34
2	Standing on O (S)	0.96	0.82	0.71	0.96	1.87	2.20
3	Line on O (A)	0.96	0.86	0.52	0.74	2.02	2.30
3	Triangle on O (B)	0.85	0.82	0.45	0.70	2.06	2.51
4	Rhombus on O (A)	0.65	1.08	0.28	0.93	2.14	2.32
4	Line on O (B)	0.80	0.89	0.39	0.81	2.02	2.59

FIG. 1. Free clusters obtained in LDA by relaxing their adsorbed geometries. Distances are in Å .

FIG. 2. Copper adsorption sites on MgO(100).

FIG. 3. LDA potential energy surface for a Cu adatom on MgO(100). Energy units are in eV and taken with respect to the lowest lying state, i.e. the copper on top of the oxygen site.

FIG. 4. Geometries of the supported Cu_n clusters. For each case, we show both the starting geometry (top or left) and the optimized structure (bottom or right).

FIG. 5. Dimer binding energy as a function of the angle θ (see text for definition) as computed in the GGA. The line is only meant as a guide for the eye.

FIG. 6. Binding energies E_{A-A} and E_{S-A} of copper clusters on MgO(100). Legends refer to the geometries of Fig. 4. GGA results are obtained through a non-selfconsistent method (see text for details).

FIG. 7. LDA density of states of free clusters. All DOS have been scaled down so that total charge is unity.

FIG. 8. LDA density of states for the adsorbed Cu_n clusters ($n = 1$ to $n = 4$ from top to bottom). All densities have been scaled down so that total charge is unity and aligned on the top of the oxygen 2s band.

FIG. 9. S, p, d projections of the DOS for a Cu adatom adsorbed at the oxygen site.

FIG. 10. LDA charge densities for a Cu adatom on top of an oxygen site. This view is along the (100) plane, containing both oxygen and magnesium atoms of the slab. Crosses denote oxygen and copper atomic positions.

FIG. 11. Density of states for a Cu adatom at the oxygen site calculated with different exchange-correlation functionals (bold line). All calculations are fully selfconsistent and include the optimization of the atomic structure. For comparison, the DOS of the clean surface (thin line) is included. The DOS have been aligned on the top of the corresponding clean surface's oxygen $2s$ band.

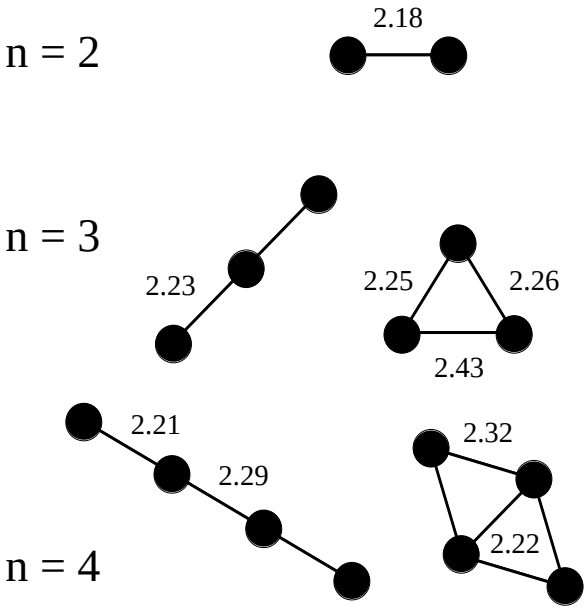

FIG. 1. Musolino *et al.*, Journal of Chemical Physics

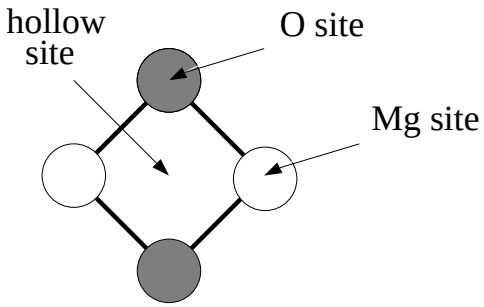

FIG. 2. Musolino *et al.*, Journal of Chemical Physics

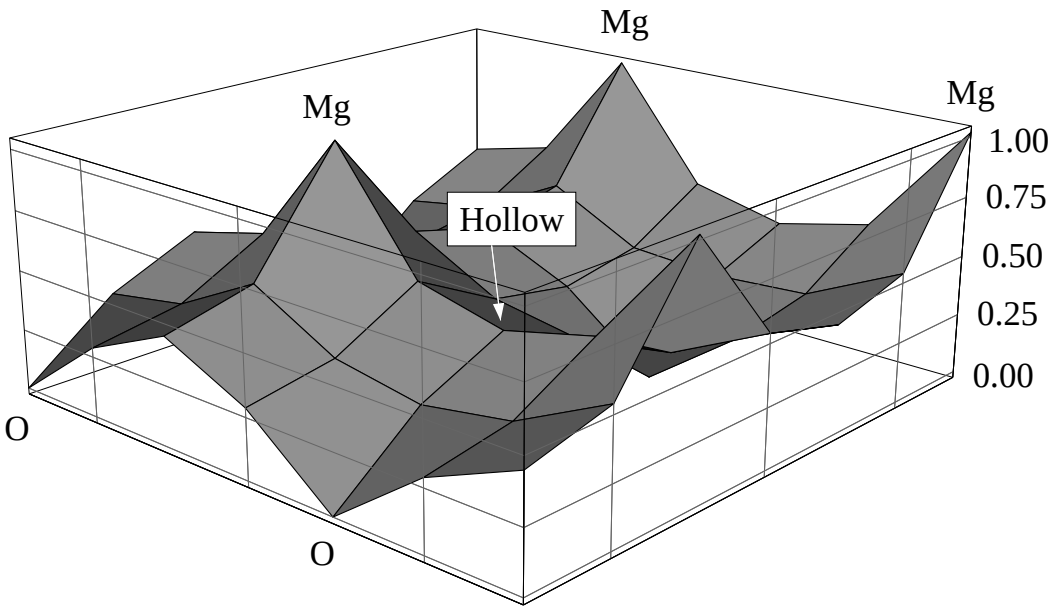

FIG. 3. Musolino *et al.*, Journal of Chemical Physics

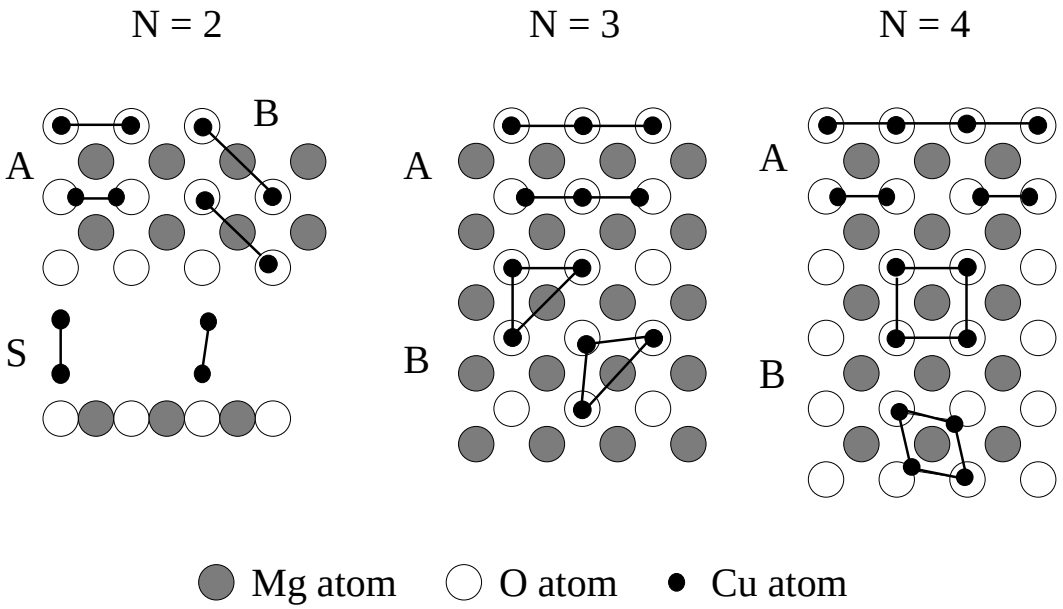

FIG. 4. Musolino *et al.*, Journal of Chemical Physics

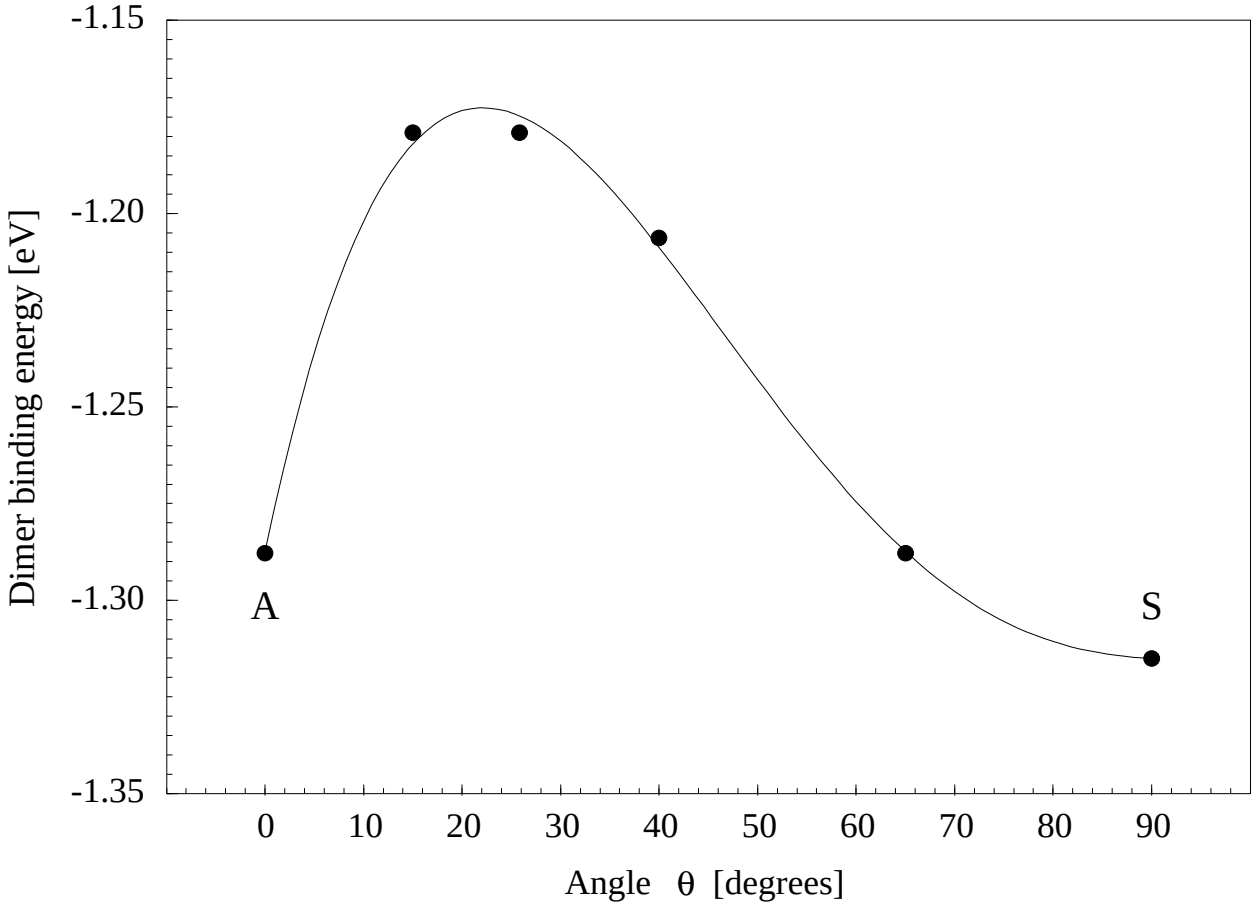

FIG. 5. Musolino *et al.*, Journal of Chemical Physics

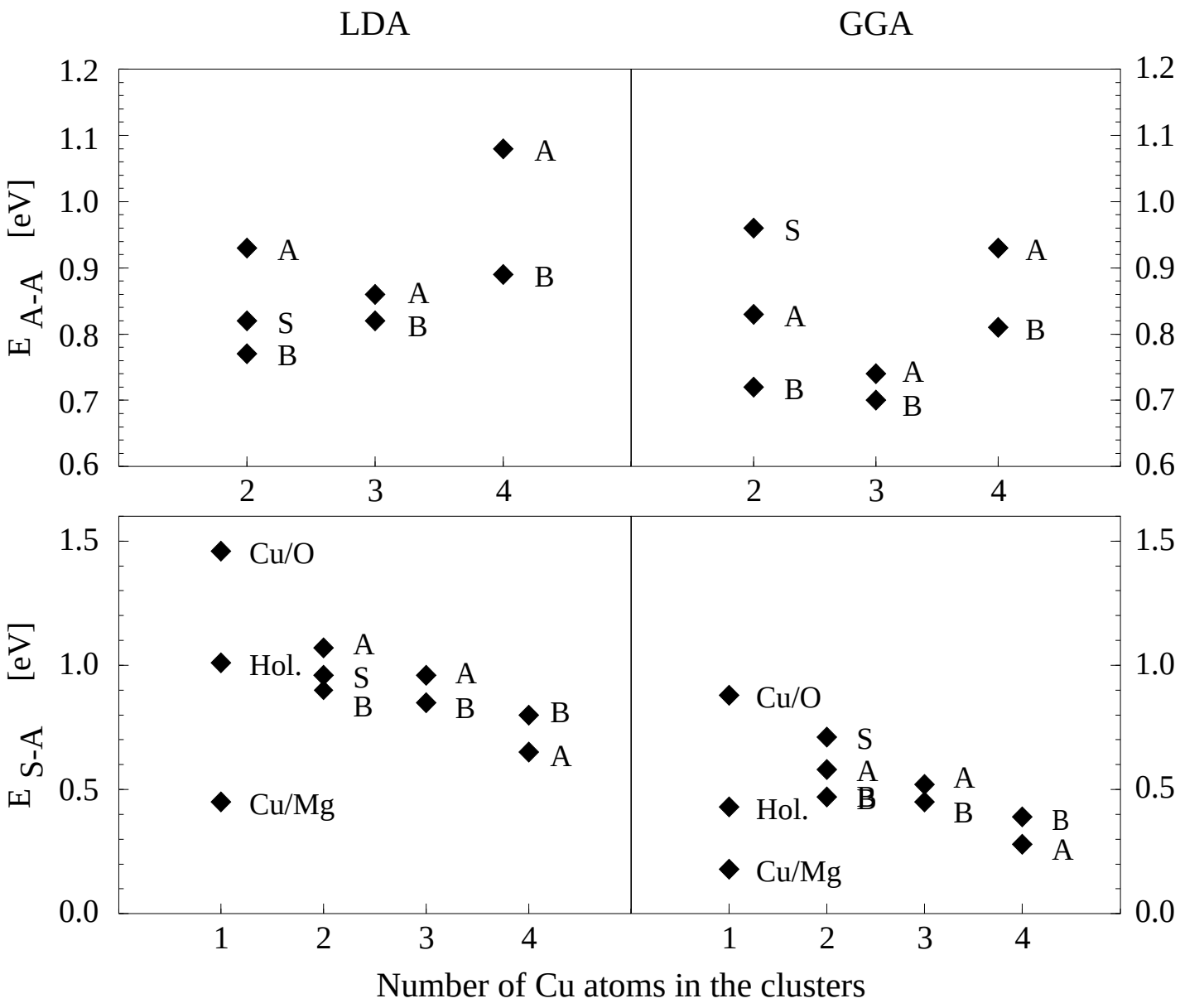

FIG. 6. Musolino *et al.*, Journal of Chemical Physics

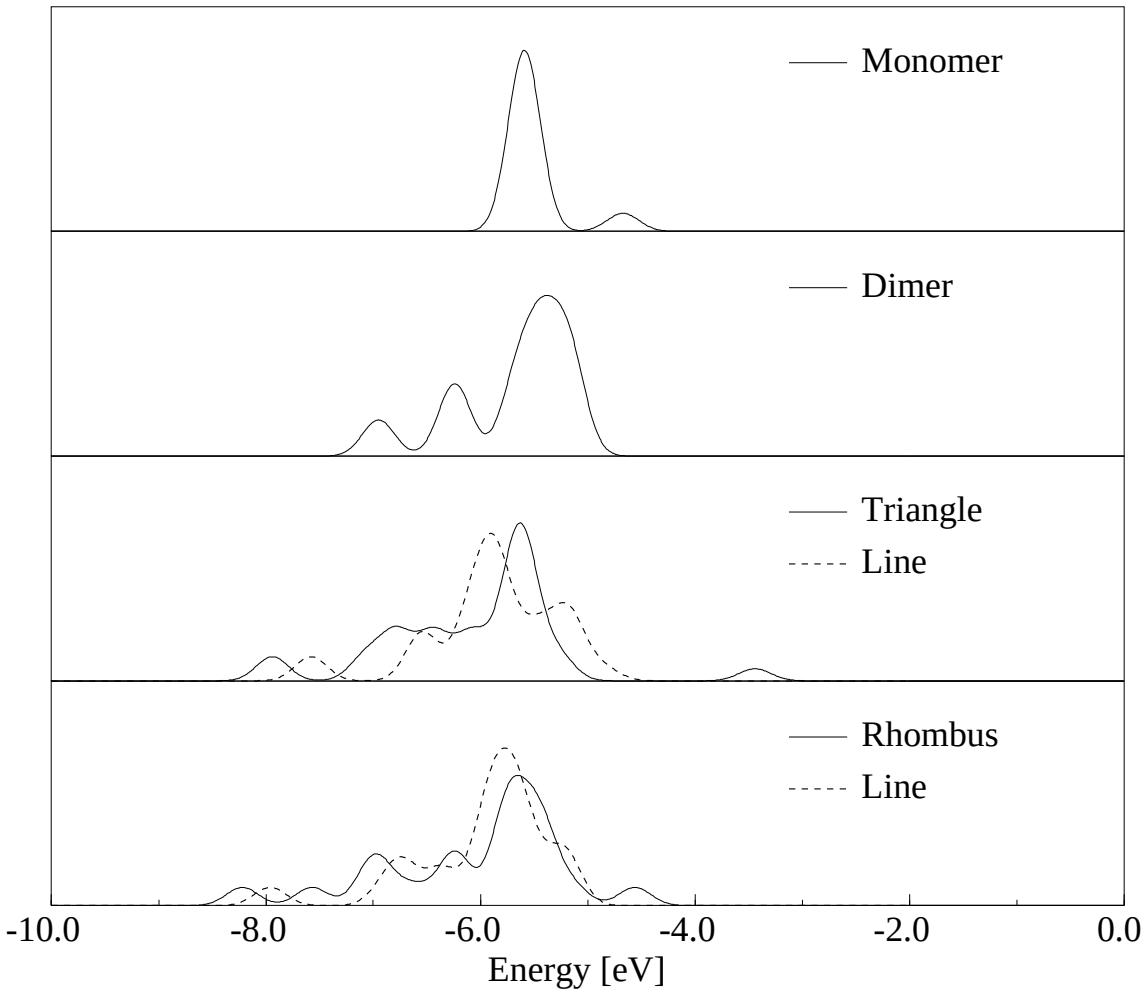

FIG. 7. Musolino *et al.*, Journal of Chemical Physics

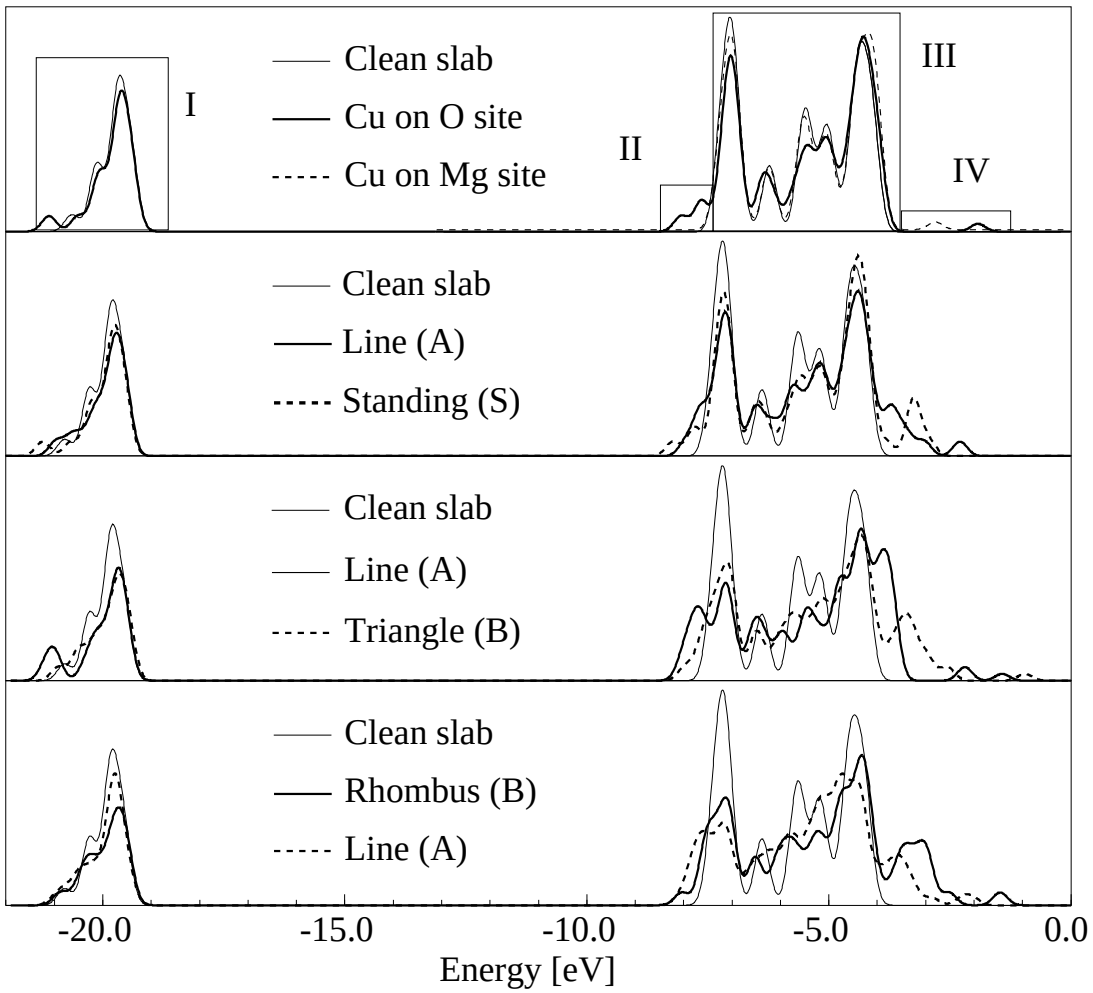

FIG. 8. Musolino *et al.*, Journal of Chemical Physics

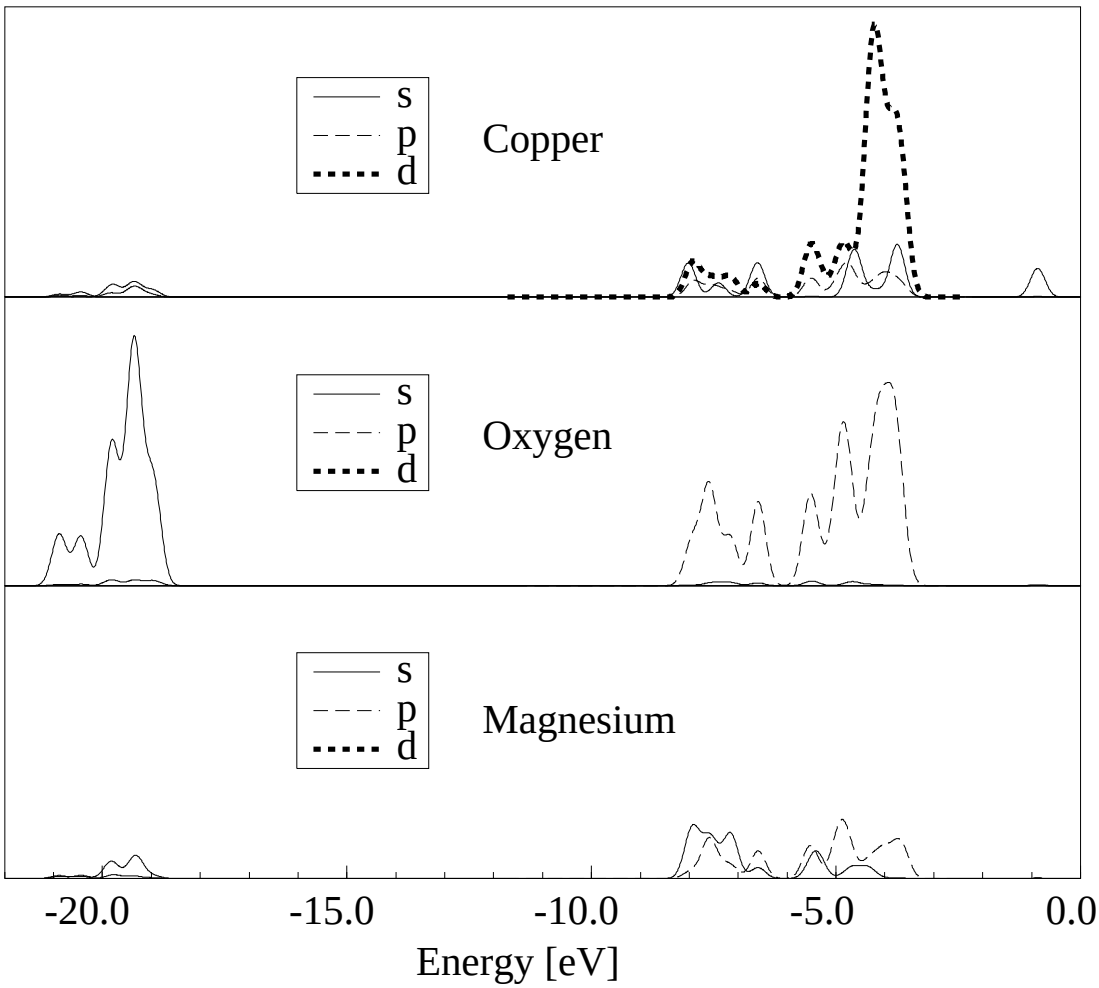

FIG. 9. Musolino *et al.*, Journal of Chemical Physics

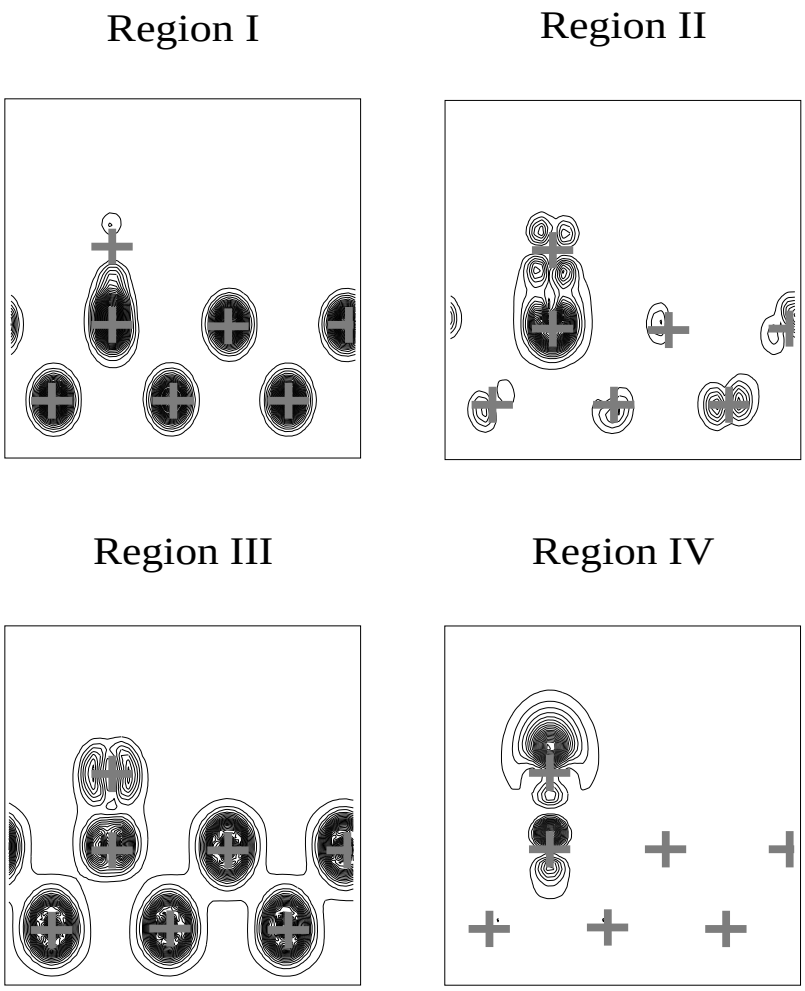

FIG. 10. Musolino *et al.*, Journal of Chemical Physics

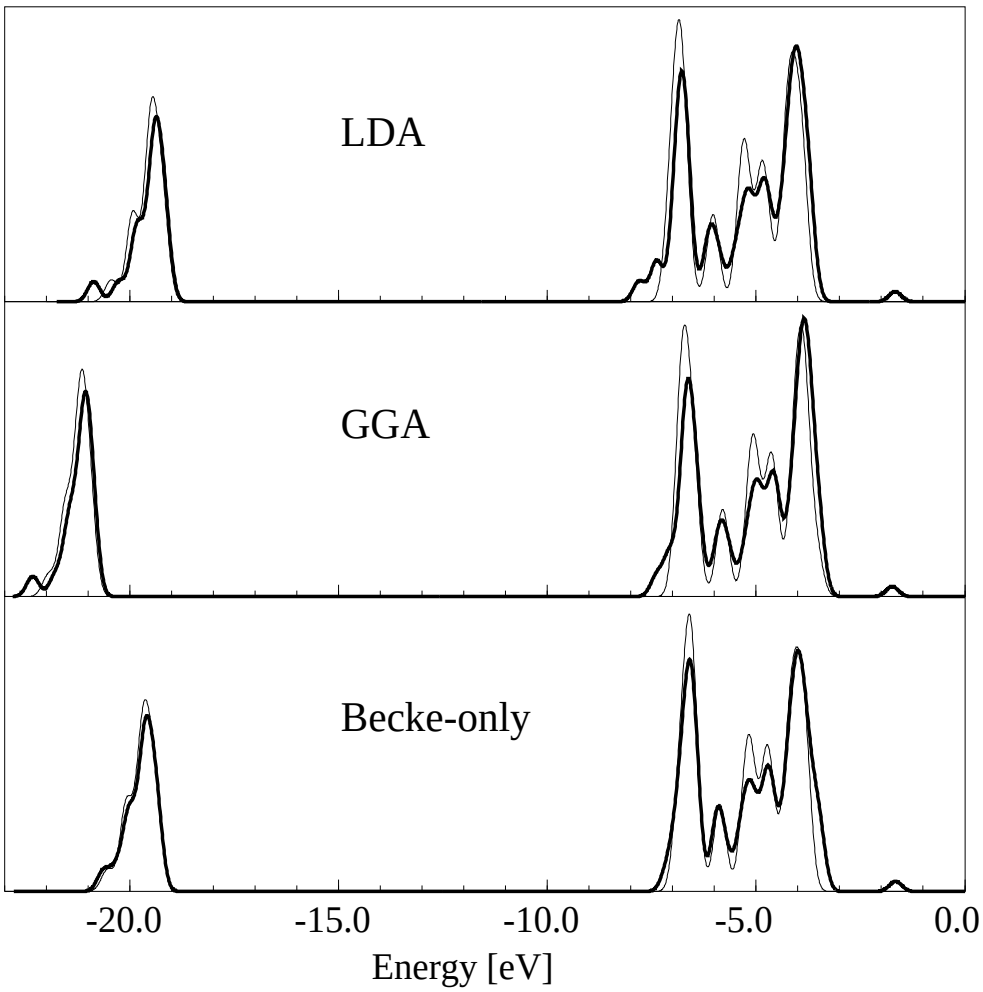

FIG. 11. Musolino *et al.*, Journal of Chemical Physics